

Supplementary Material

for

Thermodynamic stability, kinetic inertness and relaxometric properties of monoamide derivatives of lanthanide(III) DOTA complexes

*Lorenzo Tei,^a Zsolt Baranyai,^b Luca Gaino,^a Attila Forgács,^a Adrienn Vágner^b and Mauro Botta^{*a}*

^a Dipartimento di Scienze e Innovazione Tecnologica, Università del Piemonte Orientale “Amedeo Avogadro”, Viale T. Michel 11, I-15121, Alessandria, Italy

^b Department of Inorganic and Analytical Chemistry, University of Debrecen, H-4010 Debrecen, Egyetem tér 1., Hungary

Table of content:

UV-spectrophotometric studies of Ce ³⁺ - L1 system	page	1
Species distribution of Gd ³⁺ - L1 and Gd ³⁺ - L2 systems	page	2
Formation kinetics of Ln(HL1) and Ln(HL2)	page	2
Dissociation kinetics of Gd L1 and Gd L2	page	5
NMRD profile of Gd L5 at 310 K	page	7

1. UV-spectrophotometric studies of Ce^{3+} - **L1** system and the species distribution of Gd^{3+} - **L1** and Gd^{3+} - **L1** systems

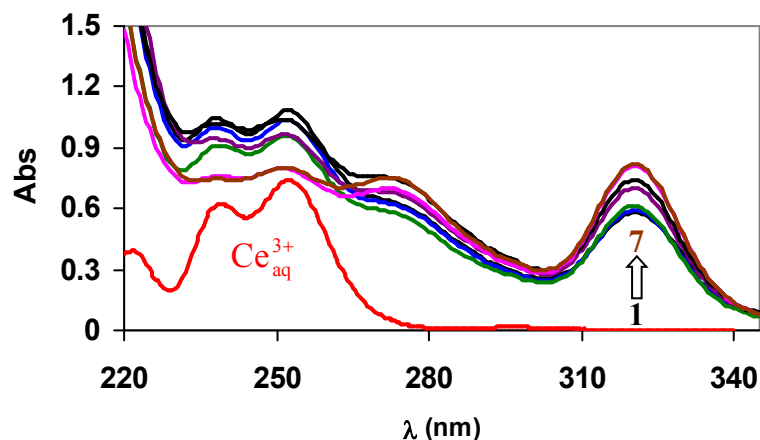


Figure S1. Absorption spectra of $\text{Ce}^{3+}_{\text{aq}}$ and Ce^{3+} - **L1** systems ($[\text{Ce}^{3+}] = [\text{DOTAEN}] = 1.5 \text{ mM}$, $\text{pH} = 2.40$ (1), 2.46 (2), 2.63 (3), 2.75 (4), 3.18 (5), 3.55 (6) and 4.20 (7), 0,1 M KCl, 298 K)

It can be seen in Figure S1 that the absorption spectra of $\text{Ce}^{3+}_{\text{aq}}$ and Ce^{3+} - **L1** systems differ considerably. In the wavelength range 300 – 340 nm, the absorbance values increase with the increase of pH due to the formation of the monoprotonated $\text{Ce}(\text{HL1})$ complex in the pH range 2.4 – 4.2. In the wavelength range 300 – 340 nm, the absorption band of the $\text{Ce}(\text{HL1})$ is characteristic for the $\text{Ce}(\text{DOTA})$ -like complexes (Burai, L.; Fabian, I.; Kiraly, R.; Szilagyi, E.; Brucher, E. *Journal of the Chemical Society, Dalton Transactions* **1998**, 243.; Baranyai, Z.; Brucher, E.; Ivanyi, T.; Kiraly, R.; Lazar, I.; Zekany, L. *Helvetica Chimica Acta* **2005**, 88, 604.) in which the Ce^{3+} -ion is placed in the coordination cage formed by the ring N and carboxylate or amide O donor atoms. Since the absorption band of the $\text{Ce}(\text{HL1})$ complexes is well separated from that of free $\text{Ce}^{3+}_{\text{aq}}$, the equilibrium studies were performed on the absorption band of $\text{Ce}(\text{HL1})$. By taking into account the molar absorptivities of $\text{Ce}(\text{HL1})$ and the protonation constant ($\log K_{\text{CeHL}}$) of the $\text{Ce}(\text{L1})$ determined by the direct pH potentiometric titration of $\text{Ce}(\text{L1})$, the stability constant of $\text{Ce}(\text{L1})$ was calculated from the absorbance values obtained at 10 wavelengths (Figure S1) in the pH range 2.4 – 4.2. The molar absorptivity values of the $\text{Ce}(\text{HL1})$ were calculated from the absorption spectra of 1.0, 2.0 and 3.0 mM $\text{Ce}(\text{HL1})$ complex recorded in the wavelength range 220 – 345 nm ($\text{pH} = 6.0$, 0.1 M KCl, 25 °C).

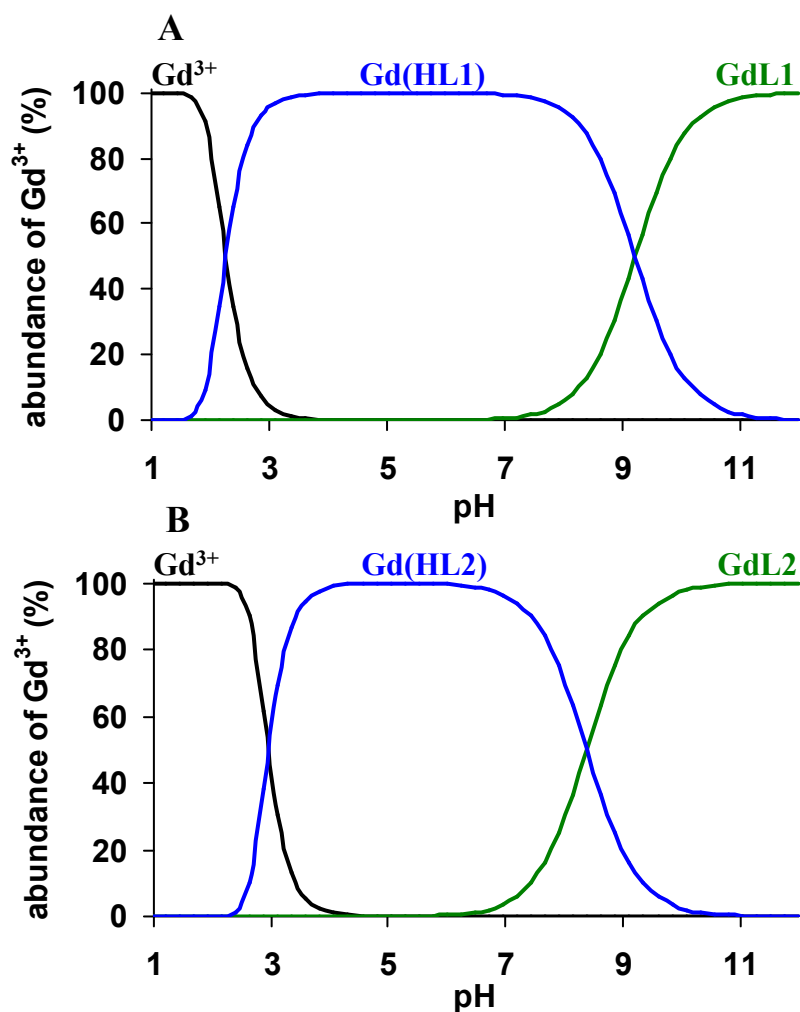


Figure S2. Species distribution of Gd³⁺ - L1 (A) and Gd³⁺ - L2 (B) systems ([Gd³⁺]=[L1]=[L2]=2.0 mM, 0.1 M KCl, 298 K)

2. Formation kinetics of Ln(HL1) and Ln(HL2):

The rates of the formation reactions of Ce(III)- and Eu(III)-complexes with L1 and L2 have been studied by spectrophotometry in the presence of 5 - 40 folds Ln(III) ion excess in the pH range 3.5 - 6.0. The absorption spectra of the Ce³⁺-L1, Eu³⁺-L1 and Ce³⁺-L2 reacting systems are shown in Figure S3 and S4.

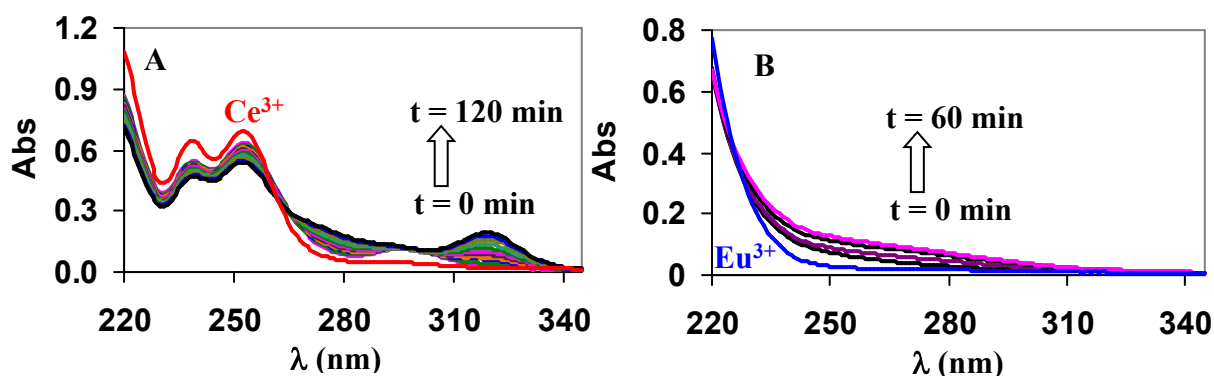


Figure S3. Absorption spectra of Ce³⁺ - L1 (A) and Eu³⁺ - L1 (B) reacting systems. ([Ce³⁺]=[Eu³⁺]=[L1]=0.001 M, [N-metil-piperazine]=0,01 M, pH=4.65, 0,1 M KCl, 25 °C)

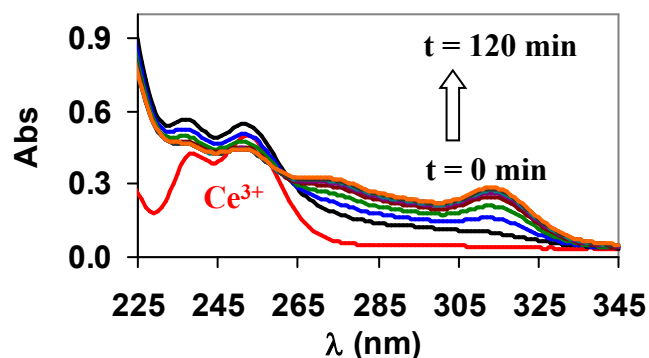


Figure S4. Absorption spectra of Ce^{3+} - L2 reacting systems. ($[\text{Ce}^{3+}] = [\text{L2}] = 0.6 \text{ mM}$, $[\text{N-metil-piperazine}] = 0.01 \text{ M}$, $\text{pH} = 4.80$, 0.1 M KCl , $25 \text{ }^\circ\text{C}$)

In the investigated pH range, $\text{Ln}(\text{HL1})$ and $\text{Ln}(\text{HL2})$ complexes predominate in which the pendant amino nitrogen is protonated. At higher pH values, the formation reactions were too fast to be followed by conventional spectrophotometry and below $\text{pH} = 3.5$ the complex formation was not complete. Under the conditions studied, the pseudo-first order rate constants (k_{obs}) obtained are shown as a function of $[\text{Ln}^{3+}]$ in Figures S5 and S6.

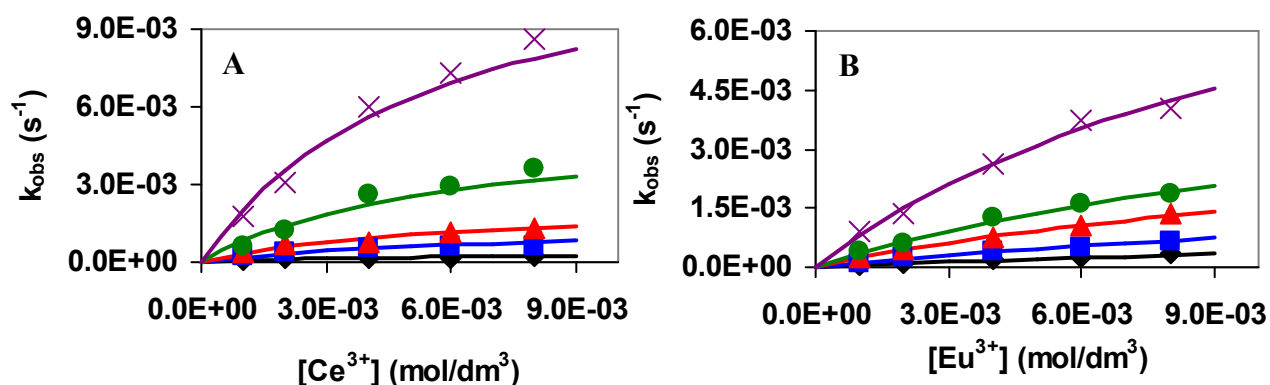


Figure S5. Pseudo-first order rate constants (k_{obs}) for the formation of $\text{Ce}(\text{HL1})$ (A) and $\text{Eu}(\text{HL1})$ (B) complexes as a function of $[\text{Ln}^{3+}]$ (A: $[\text{L}] = 2 \times 10^{-4} \text{ M}$, $\text{pH} = 4.7$ (\blacklozenge), 5.0 (\blacksquare), 5.35 (\blacktriangle), 5.65 (\bullet) and 6.0 (\times); B: $[\text{L}] = 2 \times 10^{-4} \text{ M}$, $\text{pH} = 3.8$ (\blacklozenge), 4.2 (\blacksquare), 4.5 (\blacktriangle), 4.6 (\bullet) and 4.9 (\times), $[\text{N-methyl-piperazine}] = [\text{piperazine}] = 0.01 \text{ M}$, $25 \text{ }^\circ\text{C}$, 1.0 M KCl)

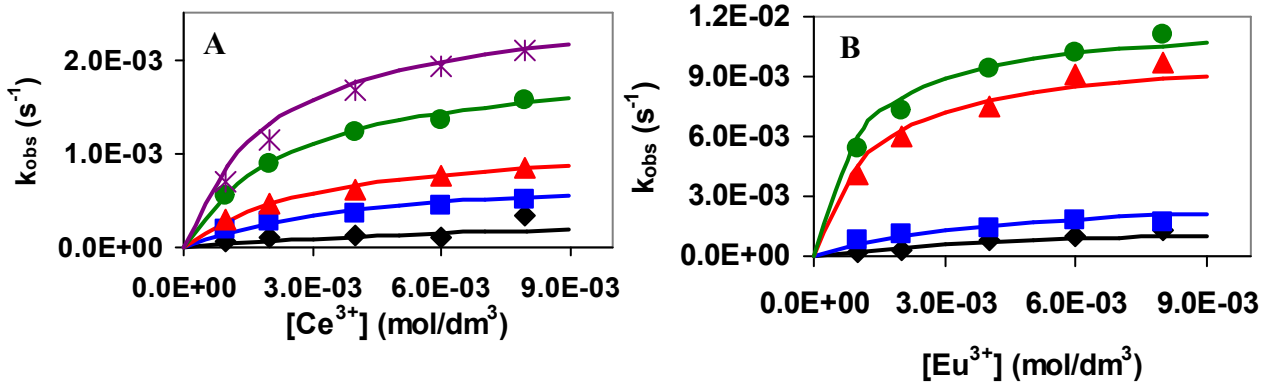


Figure S6. Pseudo-first order rate constants (k_{obs}) for the formation of Ce(HL2) (A) and Eu(HL2) (B) complexes as a function of $[\text{Ln}^{3+}]$ (A: $[\text{L}]=2 \times 10^{-4}$ M, $\text{pH}=3.85$ (\blacklozenge), 4.25 (\blacksquare), 4.45 (\blacktriangle), 4.65 (\bullet) and 4.85 (\times); B: $[\text{L}]=2 \times 10^{-4}$ M, $\text{pH}=3.60$ (\blacklozenge), 3.75 (\blacksquare), 4.40 (\blacktriangle) and 4.65 (\bullet), $[\text{N-methyl-piperazine}]=[\text{piperazine}]=0.01$ M, 25 °C, $1,0$ M KCl)

The formation rates of Ln(HL1) and Ln(HL2) complexes are expressed by Eqn. (1)

$$\frac{d[\text{LnHL}]_t}{dt} = k_{\text{obs}}[\text{L}]_t \quad (1)$$

where k_{obs} is a pseudo-first order rate constant, $[\text{L}]_t$ is the total concentration of the $\text{H}_x\text{L1}$ and $\text{H}_x\text{L2}$ ligands and $[\text{LnHL}]_t$ is the total concentration of the Ln(HL1) and Ln(HL2) complexes. Based on the similarities to the Ln^{3+} -DOTA system, the formation rate of the Ln(HL1) and Ln(HL2) complexes can be expressed by Eqn. (2):

$$\frac{d[\text{LnHL}]_t}{dt} = k_{\text{obs}}[\text{L}]_t = k_f[*\text{Ln}(\text{H}_3\text{L})] \quad (2)$$

where $*\text{Ln}(\text{H}_3\text{L})$ is the concentration of the triprotonated $*\text{Ln}(\text{H}_3\text{L})$ intermediate and k_f is the rate constant characterizing the deprotonation and rearrangement of the intermediate into LnHL complexes. By taking into account the protonation constants of L1 and L2 ($\log K_1^{\text{H}}$, Table 1), the conditional stability constants of the $*\text{Ln}(\text{H}_3\text{L})$ intermediates ($*K_{\text{Ln}(\text{H}_3\text{L})}^{\text{c}} = [*\text{Ln}(\text{H}_3\text{L})]/[\text{Ln}^{3+}][\text{H}_3\text{L}]$), the pseudo-first order rate constant can be expressed by Eqn. (3), which was used for the fitting of the k_{obs} values to determine the k_f rate constant and the stability constant ($*K_{\text{Ln}(\text{H}_3\text{L})}$) of the $*\text{Ln}(\text{H}_3\text{L})$ intermediate.

$$k_{\text{obs}} = \frac{k_f *K_{\text{Ln}(\text{H}_3\text{L})}^{\text{c}} K_1^{\text{H}} K_2^{\text{H}} K_3^{\text{H}} [\text{Ln}^{3+}][\text{H}^+]^3}{\alpha_{\text{H}} + *K_{\text{Ln}(\text{H}_3\text{L})}^{\text{c}} K_1^{\text{H}} K_2^{\text{H}} K_3^{\text{H}} [\text{Ln}^{3+}][\text{H}^+]^3} \quad (3)$$

where $\alpha_{\text{H}} = 1 + K_1^{\text{H}}[\text{H}^+] + K_1^{\text{H}}K_2^{\text{H}}[\text{H}^+]^2 + \dots + K_1^{\text{H}}K_2^{\text{H}}K_3^{\text{H}}K_4^{\text{H}}K_5^{\text{H}}K_6^{\text{H}}[\text{H}^+]^6$.

3. Dissociation kinetics of Gd(L1) and Gd(L2):

The dissociation reactions of Gd(L1) and Gd(L2) were studied by ^1H -NMR relaxometry in the $[\text{H}^+]$ range 0.05 – 1.0 M. The relaxivity values of the Gd(L1) and Gd(L2) in 0.95 M HCl as a function of time are shown in Figure S7.

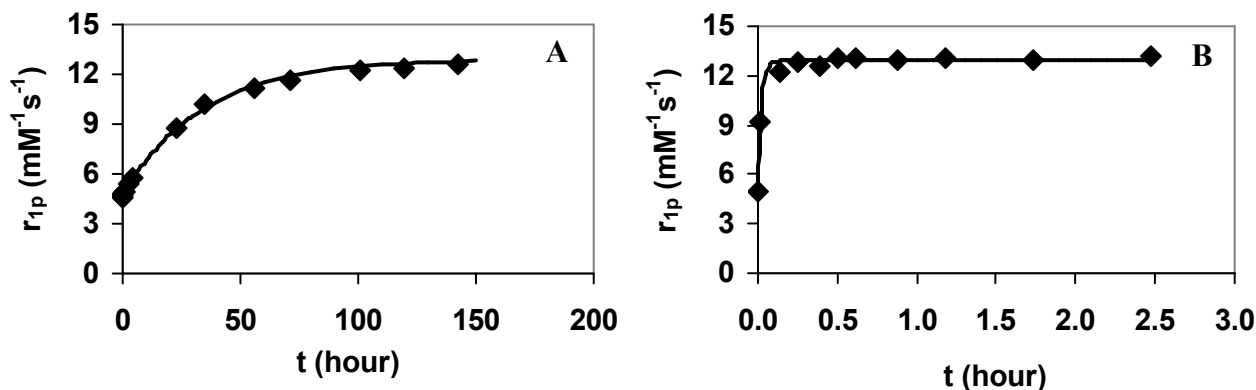


Figure S7. The relaxivity values of the Gd(L1) and Gd(L2) in 0.95 M HCl ($[\text{GdL}]=0.001$ M, $[\text{H}^+]=0.95$ M $[\text{HCl}]+[\text{KCl}]=1.0$ M, 298 K)

In the presence of excess of H^+ ion the dissociation reactions of Gd(L1) and Gd(L2) can be treated as pseudo-first-order processes and the reaction rates can be expressed with Eqn. (4), where k_d is a pseudo-first-order rate constant, $[\text{GdL}]_t$ and $[\text{GdL}]_{\text{tot}}$ are the concentrations of the GdL containing species at time t and at the beginning of the reaction.

$$-\frac{d[\text{GdL}]_t}{dt} = k_d[\text{GdL}]_{\text{tot}} \quad (4)$$

The obtained pseudo-first-order rate constants characterizing the dissociation reactions of Gd(L1) and Gd(L2) are shown in Figure S8.

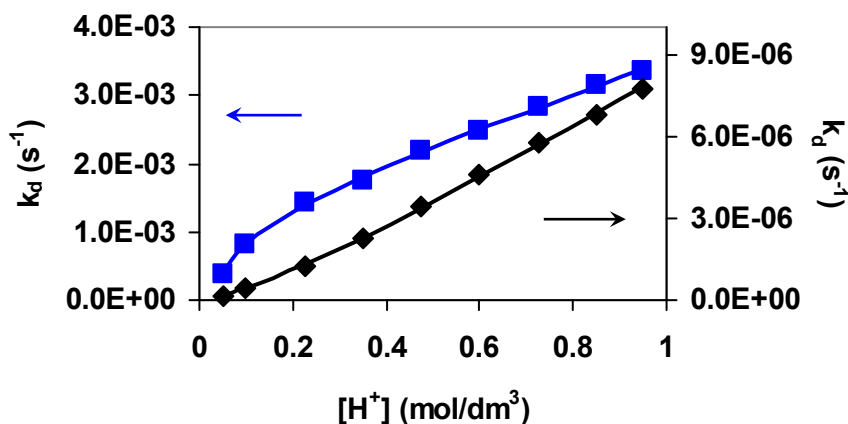
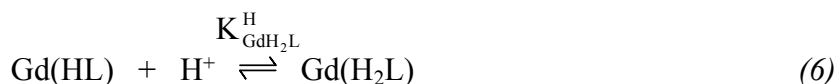


Figure S8. Pseudo-first-order rate constants (k_d) characterizing the dissociation reactions of Gd(L1) and Gd(L2) ($[\text{GdL}]=0.001$ M, $[\text{HCl}]+[\text{KCl}]=1.0$ M, 298 K)

As shown in Figure S8 the dissociation rates of Gd(L1) and Gd(L2) are proportional to $[H^+]$. The increase of k_d with increasing H^+ concentration can be interpreted in terms of the proton assisted dissociation of Gd(L1) and Gd(L2) complexes.

Considering the relatively high protonation constant of the aminoethyl group of Gd(L1) and Gd(L2) complexes (Gd(L1): $\log K_{GdHL}=9.24$; Gd(L2): $\log K_{GdHL}=8.40$), the dissociation reactions essentially occur by the spontaneous dissociation of monoprotonated Gd(HL) complexes (Eqn. (5)), by the formation (Eqn. (6)) and the dissociation of diprotonated Gd(H₂L) complexes (Eqn. (7)) and by the proton assisted dissociation of the diprotonated Gd(H₂L) complexes (Eqn. (8)).



By taking into account all the possible pathways, the pseudo-first-order rate constant (k_d) of dissociation reaction of Gd(L1) and Gd(L2) can be expressed by Eq. (9).

$$-\frac{d[GdHL]}{dt} = k_0[GdHL] + k_{GdH_2L}[GdH_2L] + k_{GdH_2L}^H[GdH_2L][H^+] \quad (9)$$

By taking into account the total concentration of the complex ($[GdL]_{tot}=[Gd(HL)]+[Gd(H_2L)]$), and the protonation constant ($K_{GdH_2L}^H$) of Gd(HL) complexes (Eqn. (6)), the pseudo-first-order rate constant (k_d) can be expressed as follows:

$$k_d = \frac{k_0 + k_1[H^+] + k_2[H^+]^2}{1 + K_{GdH_2L}^H[H^+]} \quad (10)$$

where k_0 , k_1 ($= k_{GdH_2L} \times K_{GdH_2L}^H$) and k_2 ($= k_{GdH_2L}^H \times K_{GdH_2L}^H$) are the rate constants characterizing the spontaneous and the proton-assisted dissociation of Gd(HL1) and Gd(HL2), respectively. The k_0 , k_1 , k_2 and $K_{GdH_2L}^H$ were calculated by fitting the data points presented in Figure S7 to the Eqn. (10).

4. ^1H NMRD profile of GdL5 at 310 K

